Journal of Structural Geology, Vol. 6, No. 4, pp. 417 to 423, 1984
Printed in Great Britain

0191-8141/84 $03.00 + 0.00
Pergamon Press Ltd.

A new plot to display the strain of elliptical markers

J. WHEELER

Department of Earth Sciences, University of Leeds, Leeds LS2 9JT, U.K.

(*Received* 27 *April* 1983; *accepted in revised form* 17 *October* 1983)

Abstract—A modification of the Elliott grid for plotting ellipse shape data are described. The effects of strain on elliptical markers are easy to visualize when the data are plotted on the new grid, and this allows clear interpretation of displayed data. New graphical methods for manipulating distributions of elliptical markers are directly related to an existing numerical method. When a distribution on the grid is strained, all the points move along straight, parallel lines. An initial distribution in which all the points lie on a straight line is strained into a distribution with the points lying on a hyperbola. Such curves include the analogues of 'theta curves'. If the points lie on a circle centred at the grid origin, they are strained so as to lie on an ellipse. These are the analogues of 'onion curves'.

INTRODUCTION

FOR OVER A decade, arrays of deformed ellipses, such as pebbles in conglomerates or ooliths in limestones, have been used to yield strain estimates. Early methods, for instance those of Ramsay (1967) and Dunnet (1969), involved plotting R_f, the final axial ratio, and θ_f, the angle of the major axis to a datum direction (Fig. 1), for each ellipse. The strain was estimated by superimposing sets of standard curves (often referred to as 'onion curves', which are the loci of ellipses of fixed initial axial ratio, R_i) to the plotted points, and obtaining a visual 'best fit'. Initially R_f and θ_f were plotted as Cartesian coordinates, but strain paths are difficult to visualize on the resulting diagram. Elliott (1970) proposed a much better grid, on which ln R_f was plotted as radial coordinate and $2\theta_f$ as angular coordinate. Strain was still determined by visual best fit, although the process of unstraining distributions was easier.

Later workers attempted to remove the subjectivity of this approach by inventing formal algorithms for unstraining or curve fitting. However, these tend to be complex and ambiguous. For example, Lisle (1977), presented a formal technique for fitting 'theta curves' (curves which are the loci of ellipses of fixed initial orientation, θ_i) to data. The theta curves are strained in small increments, and at each stage a statistical test is applied to test the randomness of the data relative to the curves. The result of this method is dependent on the chosen theta curve spacing, as well as the fineness of strain increments, and the computations are time consuming. Methods proposed using measurements on ellipses other than R and θ (for example Matthews *et al.* 1974, Robin 1977) have similar shortcomings.

In assessing different methods of strain analysis, there are four criteria to consider.

(1) Independent workers, applying the same method to the same data, should deduce the same strain.

(2) The method should involve no arbitrary quantities, such as the theta curve spacing in Lisle's method (see above).

(3) A rotation of the deformed marker ellipses should result in an identical rotation of the deduced strain ellipse.

(4) If a strain **E** has been deduced from a set of data, and that data is deformed by deformation **D** by direct computation, then the strain deduced from the new data should be that corresponding to the resultant deformation **DE**. Any method satisfying (4) will satisfy (3) but the converse is not always true.

Most methods conform empirically to these criteria, but with appropriate data will violate one or more of them. The only method which uses only the shapes of marker ellipses, and can be proved to satisfy the above criteria, is that of Shimamoto & Ikeda (1976). In itself this would seem to be sufficient, and it involves no pictorial representation of the data. There are several reasons why a related graphical technique is necessary.

(1) If a computer is not available, a strain estimate can still be made.

(2) Strain paths can be constructed quickly.

(3) Other features in the rock such as bedding and cleavage, can be visualized in relation to the distribution.

(4) When displayed graphically the undeformed distribution may not look random, for which there are six possible explanations.

(a) The initial distribution did not satisfy the randomness criterion. In this case it might have been an initial sedimentary clast pattern (see Elliott 1970).

(b) The initial distribution satisfied the randomness criterion but was asymmetric in some way.

(c) The sample size is too small, in which case a sample taken from a random population may look non-random.

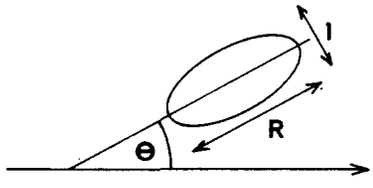

Fig. 1. The definition of R and θ for an ellipse.

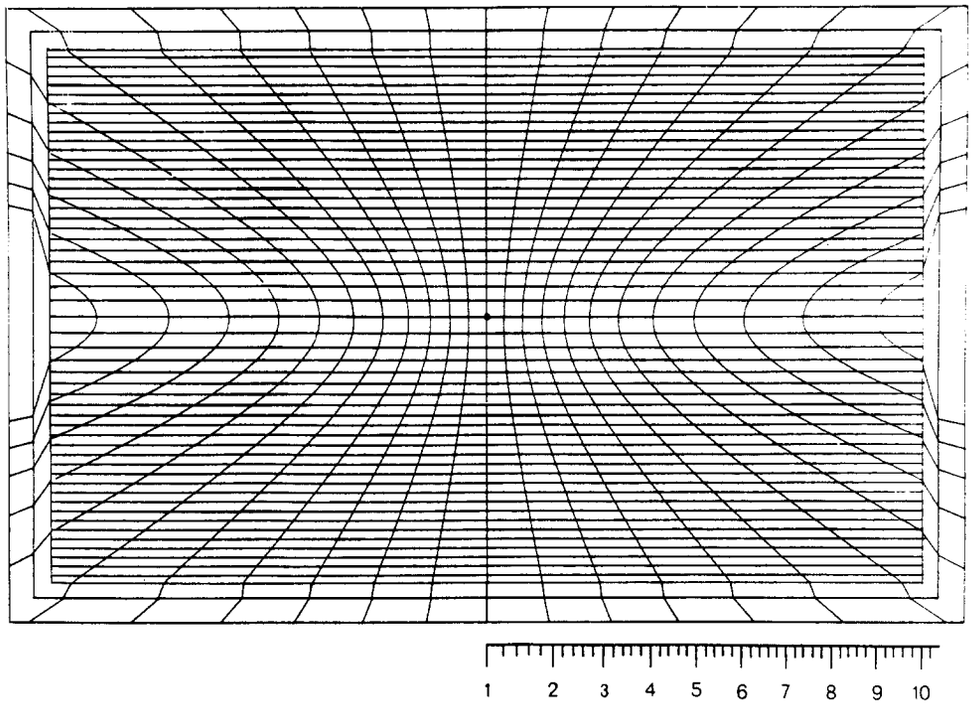

Fig. 2. The modified Elliott grid. The scale shows the radius in terms of R. Increment in R along Y-axis is 0.2: increment in ln R for hyperbolae is 0.2. See text for details of use.

(d) A few anomalous data points are responsible, which may be the result of measurement error.

(e) The assumption that markers, matrix and bulk rock all suffer the same strain is incorrect.

(f) The bulk strain varied across the sample.

There is a simple modification to the Elliott grid which gives a direct link to the Shimamoto & Ikeda (1976) method, and has additional useful properties. The proposed modification to the Elliott (1970) plot (Fig. 2) involves plotting

$$\sinh 2\epsilon = \tfrac{1}{2}(R - 1/R) \qquad (1)$$

as the radial coordinate, instead of ϵ. Equations (A1)–(A27) cited in the following discussion are given in the Appendix.

GRAPHICAL USES

Ellipses, whether they are initial or final shapes, or are themselves strain ellipses, are plotted as follows: the angle θ is doubled and then measured anticlockwise from the datum to give the ray on which the point will lie. The radius is determined from the scale (Fig. 2), and must, of course, be measured from $R = 1$ at the origin. Alternatively the radius

$$\tfrac{1}{2}(R - 1/R) \qquad (2)$$

can be calculated directly.

Once plotted, points can be strained as follows: orientate the grid until the required long axis at the strain ellipse is along the X-axis. Then to strain a point, move it to the right along the coaxial strain path, a straight line parallel to the X-axis (on the Elliott (1970) grid, corresponding paths are curved). The hyperbolae (which are the loci of ellipses for which θ_i was $\pm 45°$) are separated by constant ln R increments of 0.2. To strain a point by, for example, ln $R = 0.6$, move the point 3 hyperbolae to the right.

If we have a set of points which initially lay on a circle round the origin (R_i constant), these are deformed into an ellipse, whose long axis points along the axis of strain. Concentric circles give non-concentric ellipses (Fig. 3) but all the ellipses have the same axial ratio. It must be emphasized that this is not the axial ratio of the strain ellipse, but is simply related to it (equation A15). These ellipses are the analogues of the 'onion curves' of Dunnet (1969). The set of non-concentric ellipses for a given imposed strain will hence be referred to as an 'onion set'. Each onion curve is now an 'onion-ellipse'.

To determine the strain in a distribution of elliptical markers, plot the distribution on the grid. If an onion set can be fitted, then the strain is that of the onion set. If an onion set cannot be fitted then the distribution was not initially random. If onion sets are not available, a single onion-ellipse can be drawn by hand to enclose the bulk of the distribution. The two ends of the onion-ellipse will give representative values for the maximum and minimum final axial ratios of the elliptical markers. These values can be read off using the radial scale on the grid (Fig. 2). The strain ratio will be the harmonic mean of the maximum and minimum final axial ratios. To check on this, compare the axial ratio of the enveloping onion-ellipse with that derived from equation (A15), which relates the strain ratio to the axial ratio to the onion-ellipse. Other ellipses can be drawn inside the

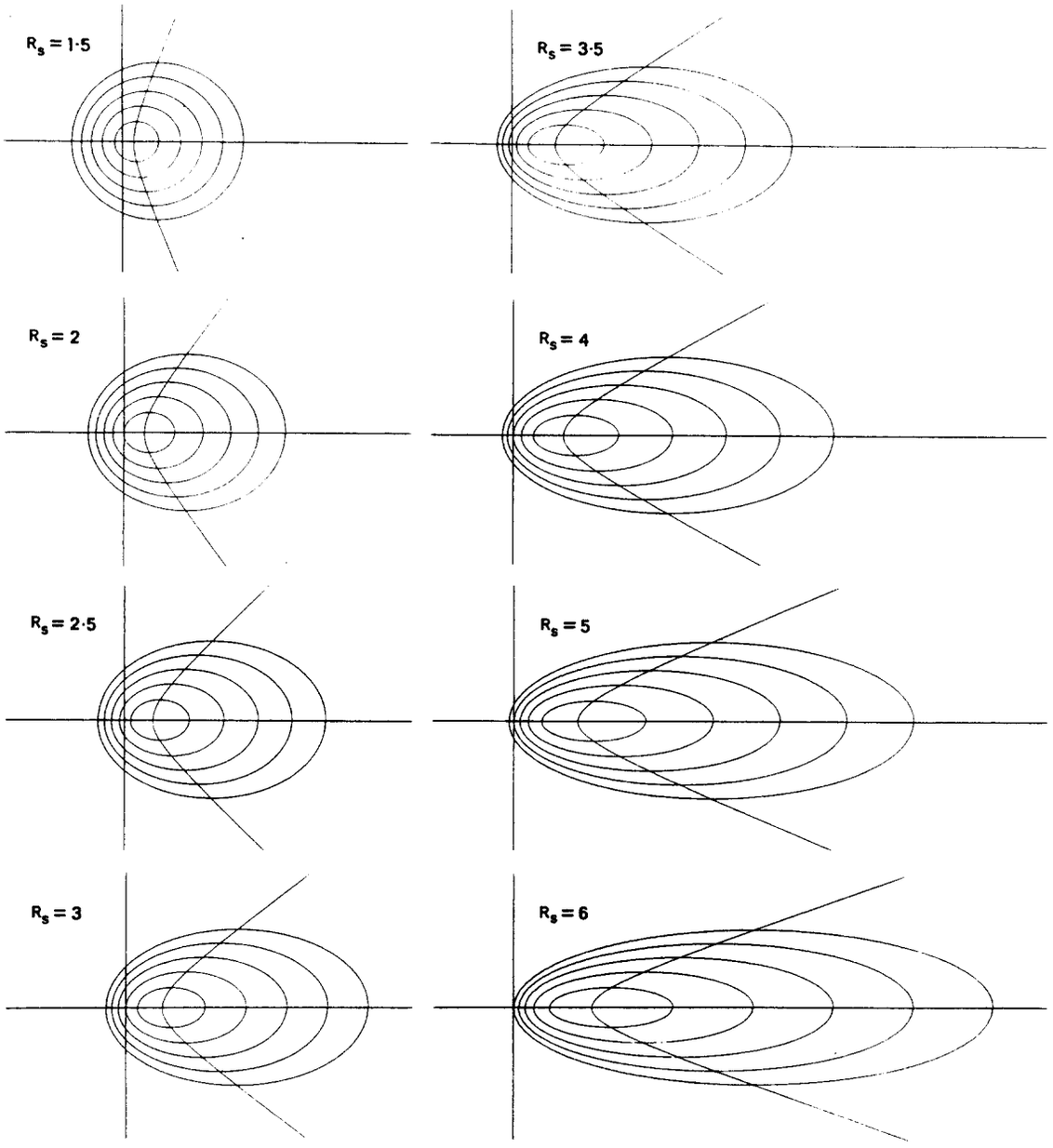

Fig. 3. Onion sets for various strain ratios. For each set, initial ratios of R_i = 1 to 6 are illustrated. The hyperbolae are the images of the Y-axes.

envelope and compared qualitatively with the onion set shapes in Fig. 3.

In this context it is worth noting that 'contours' (defined as being lines of constant point density) do not necessarily deform in the same way as the points which they contour. For instance, points on the right-hand side of the grid will become rarefied as strain occurs, whereas on the left-hand side they will be condensed. So though they may lie on the same contour to begin with, they will end up on different ones. This aspect is illustrated in Fig. 4 in which a model initial distribution, of constant density on the grid, is deformed.

Bedding planes should be represented by points at infinity on the plot, since they are geometrically equivalent to infinitely flattened ellipses. Instead they are represented by ticks round the outer margin of the grid, each tick at an angle 2θ to the plot axis, the angle of bedding to the reference direction in real space being θ (Fig. 2). The ticks point towards the theoretical location of the infinity point. Note that each bedding plane or other linear feature corresponds to only one tick and not a pair of diametrically opposed ticks. Each tick is also the asymptote to one of the hyperbolae, because as ellipse points move with the hyperbolae, bedding directions move with the asymptotes (equations A26 and A27). Consider the example above, in which points representing ellipses moved 3 hyperbolae to the right. Then any bedding or other passively deforming linear feature will move 3 ticks to the right. This procedure is identical to using the Elliott plot to deform linear features.

An example of a set of deformed ellipses has been chosen from the Pipe Rock (Cambrian) of Northwest Scotland, and is shown in Fig. 5(a). The markers are the bedding-plane intersections of worm tubes, and there has been bedding-parallel strain. The onion set has been calculated from the result of the Shimamoto & Ikeda

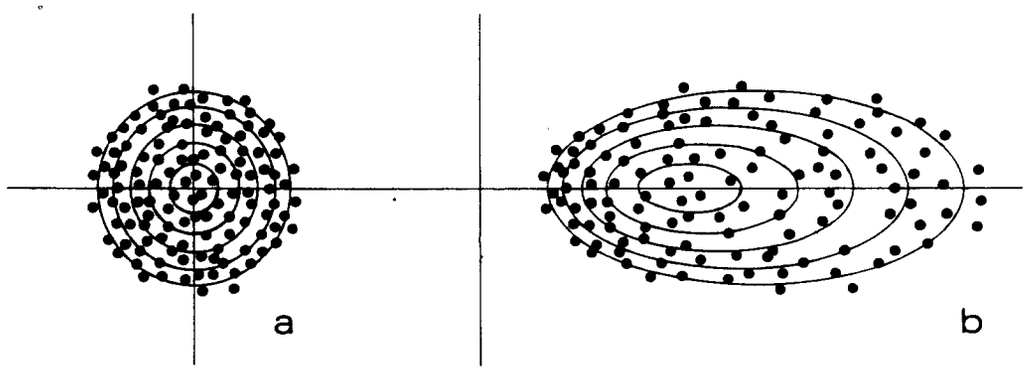

Fig. 4. A simulated random distribution, unstrained in (a) and subject to a strain of $R_s = 4$ in (b). In the unstrained state the point density on the new grid is constant; in the strained state it is not. Hence, though onion-ellipses may be density contours in an ideal initial random distribution, this will not be true after strain.

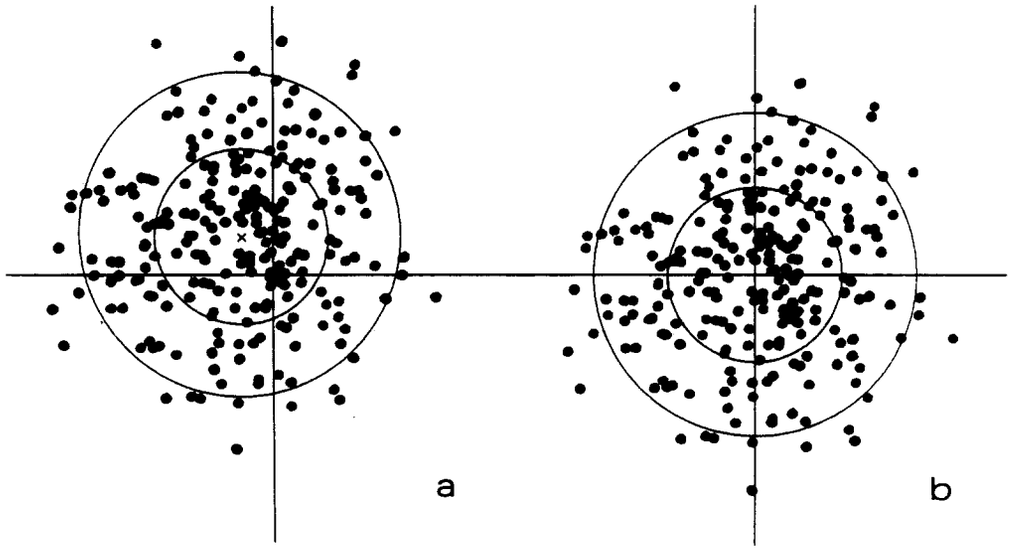

Fig. 5. (a) Pipe data plotted on the new grid. Points denote ellipse shapes, and the cross denotes the strain ellipse, which has $R_s = 1.13$ at 65.1 degrees. An onion set has been superimposed, with R_i increments of 0.25, the largest R_i being 1.5. (b) The same data, restored to the unstrained state, with the onion set also restored.

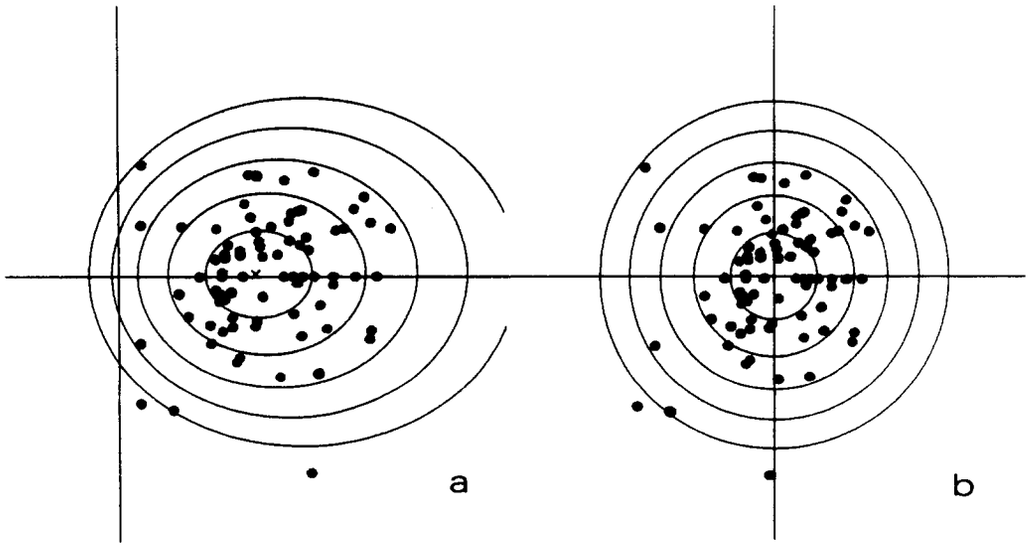

Fig. 6. Additional pipe data, (a) strained and (b) unstrained. The strain is $R_s = 1.93$ at 0.5 degrees. Onion set increments of 0.25.

(1976) method, and illustrates what a best fit ought to look like. In Fig. 5(b), the distribution has been restored to its original shape, and the onion set restored to the zero-strain onion set (i.e. concentric circles). It should be noted that the process of 'restoring' or 'unstraining' a distribution simply involves imposing an additional strain $(1/R_s, \theta_s)$ on a distribution which has suffered a strain (R_s, θ_s), and there is no technical distinction between straining and unstraining.

The unstrained distribution in Fig. 5(b) shows random scatter about the origin as one would expect. Figure 6 shows a similar set of pipes, strained and unstrained. The unstrained distribution in Fig. 6(b) is not ideally random; there are about five points on the left which have anomalously high apparent initial ellipticity, and low final ellipticity. This might indicate that pipes of different initial shapes have deformed differently, those of higher initial ellipticity being rotated as well as strained, those of low ellipticity less affected by rotation. Alternatively the anomalies could be simply a result of the sampling process, small samples from a random population are not in general random. Whatever the explanation, the use of the plot illuminates features which would otherwise escape attention.

NUMERICAL ASPECTS

The 'average strain' is defined by equations (A19)–(A21). The point at which this strain ellipse plots on the grid lies on the line connecting the centroid of the distribution to the origin, but is closer to the origin than is the centroid, by a factor J. A random distribution thus has its centroid at the origin, as one would expect intuitively. It is worth noting that equation (A18) is not the only possible criterion for randomness, but is the most amenable to mathematical treatment. Note also that the objectivity of the method is more important than its apparent accuracy. The 'distribution spread invariant' (J) is a measure of the spread of axial ratios in the initial distribution: it should be near unity for, for instance, nearly circular ooliths, but will be more for conglomerates with some initially elongate clasts. The latter correspond to Elliott's (1970) 'delta' and 'heart' distributions. It is suggested that J could be used to discriminate between different sorts of initial distribution, whether or not they are deformed. Distributions of low J are better for deducing strains.

DISCUSSION

The new grid reflects the actual geometry of deforming ellipses in a very direct way. Hence it should shed light on the problem areas of strain analysis.

(1) The deformed ellipse distribution in some sediments is not symmetric about the cleavage, which it must be if the cleavage is a principal plane of the finite strain ellipse and the initial distribution was random. The solution is often taken to be that the initial distribution was non-random but symmetric with respect to bedding. There exists a simple objective numerical solution in this situation, along the lines of the Shimamoto & Ikeda (1976) method.

(2) There has been disagreement about whether the strain history of the sample (coaxial or non-coaxial) affects the finite strain deduced using existing methods (Siddans 1980, De Paor 1981). Equation (A21) shows that the strain history nowhere enters the method, and does not affect the result.

(3) The method gives a value of the apparent finite strain suffered by the marker ellipses. This is the same as the bulk strain only if the ellipses and matrix deformed homogeneously and there was no ductility contrast. It remains for the work of Gay (1968) to be applied in this context.

Acknowledgements—I thank members of the Department of Earth Sciences at Leeds for useful discussion, and Richard Morgan and Phil Nell for providing the pipe strain data.

REFERENCES

De Paor, D. G. 1981. Elliptical markers and non-coaxial strain increments—discussion. *Tectonophysics* **75**, 335–340.
Dunnet, D. 1969. A technique of finite-strain analysis using elliptical particles. *Tectonophysics* **7**, 117–136.
Elliott, D. 1970. Determination of finite strain and initial shape from deformed elliptical objects. *Bull. geol. Soc. Am.* **81**, 2221–2236.
Gay, N. C. 1968. Pure shear and simple shear deformation of inhomogeneous viscous fluids—I. Theory. *Tectonophysics* **5**, 211–234.
Harvey, P. K. & Laxton, R. R. 1980. The estimation of finite strain from the orientation distribution of passively deformed linear markers: eigenvalue relationships. *Tectonophysics* **70**, 285–307.
Lisle, R. J. 1977. Clastic grain shape and orientation in relation to cleavage from the Aberystwyth Grits, Wales. *Tectonophysics* **39**, 381–395.
Matthews, P. E., Bond, R. A. B. & Van Den Berg, J. J. 1974. A new method of strain analysis using elliptical markers. *Tectonophysics* **24**, 31–67.
Means, W. D. 1976. *Stress and Strain*. Springer, New York.
Ramsay, J. G. 1967. *Folding and Fracturing of Rocks*. McGraw-Hill, New York.
Robin, P-Y. F. 1977. Determination of geologic strain using randomly oriented strain markers of any shape. *Tectonophysics* **42**, T7–T16.
Shimamoto, T. & Ikeda, Y. 1976. A simple algebraic method for strain estimation from deformed ellipsoidal objects—I. Basic theory. *Tectonophysics* **36**, 315–337.
Siddans, A. W. B. 1980. Elliptical markers and non-coaxial strain increments. *Tectonophysics* **67**, T21–T25.
Woodcock, N. H. 1977. Specification of fabric shapes using an eigenvalue method. *Bull. geol. Soc. Am.* **88**, 1231–1236.

APPENDIX

Notation

g unit tensor
D deformation tensor
F Finger's tensor = $\mathbf{DD}^{\mathrm{T}}$
N shape tensor = $\mathbf{F}(\det \mathbf{F})^{-1/2}$
E strain tensor = $\mathbf{F}^{1/2}$
R rotational part of deformation, such that

$$\mathbf{RR}^{\mathrm{T}} = \mathbf{g} \quad \text{and} \quad \mathbf{D} = \mathbf{ER}$$

R axial ratio of ellipse
$\eta = \ln R$
$\epsilon = \eta/2$
θ angle of ellipse to x-axis
$\alpha = 2\theta$

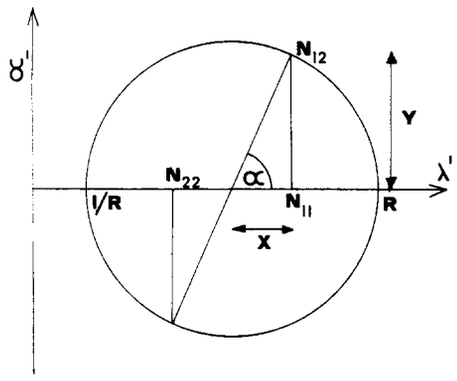

Fig. 7. The relation of the new grid vector (X, Y) to the conventional Mohr diagram.

X, Y Cartesian coordinates on grid
$\mathbf{P}$ the grid vector (X, Y)
J distribution spread invariant
i, s, f subscripts denoting initial, strain, final
av(q) average of any set of quantities q.

The result of two deformations $\mathbf{D}_1$ and $\mathbf{D}_2$ is given by

$$\mathbf{D} = \mathbf{D}_2\mathbf{D}_1 \tag{A1}$$

so

$$\mathbf{F} = \mathbf{D}_2\mathbf{D}_1(\mathbf{D}_2\mathbf{D}_1)^{\mathrm{T}} = \mathbf{D}_2\mathbf{F}_1\mathbf{D}_2^{\mathrm{T}}. \tag{A2}$$

It is possible to consider this not as a superimposition of two deformations, but as a deformation $\mathbf{D}_2$ of an initial ellipse given by $\mathbf{F}_1$—whose equation would be

$$\mathbf{x}.\mathbf{F}_1^{-1}\mathbf{x} = 1. \tag{A3}$$

We are interested only in the shapes of ellipses. Defining the shape tensor, $\mathbf{N}$, by

$$\mathbf{N} = \mathbf{F}(\det \mathbf{F})^{-1/2} \tag{A4}$$

we have

$$\det \mathbf{N} = 1. \tag{A5}$$

Then for an ellipse oriented along the x-axis

$$\mathbf{N} = \begin{bmatrix} R & 0 \\ 0 & 1/R \end{bmatrix}. \tag{A6}$$

If the ellipse axis is at angle θ to the x-axis, then we can derive its shape tensor by subjecting the tensor of (A6) to a purely rotational deformation through angle θ. The deformation matrix is then

$$\mathbf{R} = \begin{bmatrix} \cos\theta & -\sin\theta \\ \sin\theta & \cos\theta \end{bmatrix}$$

which we use in (A2) to obtain

$$\mathbf{N} = \tfrac{1}{2}\begin{bmatrix} (R + 1/R) + (R - 1/R)\cos 2\theta, & (R - 1/R)\sin 2\theta \\ (R - 1/R)\sin 2\theta, & (R + 1/R) - (R - 1/R)\cos 2\theta \end{bmatrix}. \tag{A7}$$

This may be compared with equation (3-72) of Ramsay (1967). It is convenient to introduce alternative representations to R and θ as follows:

$$\begin{aligned} X &= \sinh\eta\cos\alpha = \tfrac{1}{2}(\mathrm{N}_{11} - \mathrm{N}_{22}) \\ Y &= \sinh\eta\sin\alpha = \mathrm{N}_{12} \end{aligned} \tag{A8}$$

X and Y are Cartesian coordinates on the grid, $\sinh\eta$ is the radial coordinate and α is the angular coordinate. Substituting (A8) in (A7),

$$\mathbf{N} = \begin{bmatrix} \cosh\eta + \sinh\eta\cos\alpha, & \sinh\eta\sin\alpha \\ \sinh\eta\sin\alpha, & \cosh\eta - \sinh\eta\cos\alpha \end{bmatrix} \tag{A9}$$

$$= \begin{bmatrix} \sqrt{1 + X^2 + Y^2} + X, & Y \\ Y, & \sqrt{1 + X^2 + Y^2} - X \end{bmatrix}. \tag{A10}$$

So far formulae have concerned any ellipse, be it a marker shape or a strain ellipse. In what follows, $\mathbf{N}_f$ refers to a final marker shape, $\mathbf{N}_i$ to the initial marker shape, and $\mathbf{N}_s$ to the strain ellipse. Superimpose a pure shear, axial ratio R_s, on the ellipse. So

$$\mathbf{D}_s = \begin{bmatrix} \sqrt{R_s} & 0 \\ 0 & 1/\sqrt{R_s} \end{bmatrix}$$

and, with (A2),

$$\begin{aligned} \mathbf{N}_f &= \mathbf{D}_s\mathbf{N}_i\mathbf{D}_s^T \\ &= \begin{bmatrix} R_s(\mathbf{N}_i)_{11}, & (\mathbf{N}_i)_{12} \\ (\mathbf{N}_i)_{12}, & (\mathbf{N}_i)_{22}/R_s \end{bmatrix} \end{aligned}$$

which can be recast in terms of X and Y:

$$\begin{aligned} X_f &= X_i\sqrt{1 + X_s^2} + \sqrt{1 + X_i^2 + Y_i^2}\,X_s \\ Y_f &= Y_i \end{aligned} \tag{A11}$$

or in terms of η and α,

$$\cosh\eta_f = \cosh\eta_i\cosh\eta_s + \sinh\eta_i\sinh\eta_s\cos\alpha_i$$

$$\tan\alpha_f = \frac{\sinh\eta_i\sin\alpha_i}{\cosh\eta_i\sinh\eta_s + \sinh\eta_i\cosh\eta_s\cos\alpha_i} \tag{A12}$$

(these equations were misprinted in Elliott 1970).

The diagram has the following properties.

(a) As R_s increases, Y stays constant. So if we represent the ellipse by Cartesian coordinates X, Y, coaxial paths will be straight, parallel lines.

(b) On the Mohr diagram (Fig. 7), the vector (X, Y) has a simple meaning.

(c) The properties of the plot are rotationally invariant. So (a) is true for all strain orientations.

(d) The diagram is similar to the Elliott (1970) plot except that instead of plotting

$$\epsilon = \eta/2$$

as radius, we plot

$$\sqrt{X^2 + Y^2} = \sinh\eta = \tfrac{1}{2}(R - 1/R)$$

(see eqns A8).

The line $X_i = 0$ becomes deformed into true hyperbolae given by

$$X_f = X_s\sqrt{1 + Y_f^2}. \tag{A13}$$

Circles $X_i^2 + Y_i^2 = A^2$ (corresponding to distributions of fixed R_i) become deformed to ellipses

$$\left(\frac{X_f - \sqrt{1 + A^2}\,X_s}{\sqrt{1 + X_s^2}}\right)^2 + Y_f^2 = A^2 \tag{A14}$$

which have an axial ratio

$$\sqrt{1 + X_s^2} = \cosh\eta_s = \tfrac{1}{2}(R_s + 1/R_s). \tag{A15}$$

Now consider eqn. (A2):

$$\mathbf{F}_f = \mathbf{D}_s\mathbf{F}_i\mathbf{D}_s^{\mathrm{T}}$$

so

$$\det\mathbf{F}_f = (\det\mathbf{D}_s)^2\det\mathbf{F}_i$$

and

$$\mathbf{N}_f = \frac{1}{\det\mathbf{D}_s}\mathbf{D}_s\mathbf{N}_i\mathbf{D}_s^{\mathrm{T}}. \tag{A16}$$

The following method is a slight modification of that of Shimamoto & Ikeda (1976)—they use $\mathbf{N}^{-1}$ instead of $\mathbf{N}$, but results are equivalent. It uses the concept of an 'averaged tensor'. The average of a set of tensors is obtained by adding them together and dividing by their number, in the usual way. The tensor average is not a new concept. It has been used implicitly in the literature for the calculation of a tensor used to describe the overall geometry of sets of planes or lines. This is 'Scheidegger's orientation tensor' (Woodcock 1977), also referred to as the 'dispersion matrix' (Harvey & Laxton 1980). Consider a direct average of all the shape tensors

$$\mathrm{av}\,(\mathbf{N}_f) = \frac{1}{\det\mathbf{D}_s}\mathbf{D}_s\,\mathrm{av}\,(\mathbf{N}_i)\mathbf{D}_s^{\mathrm{T}} \tag{A17}$$

since $\mathbf{D}_s$ is assumed homogeneous. This suggests that we could define a 'randomness criterion' for ellipses by

$$\mathrm{av}\,(\mathbf{N}_i) = J\mathbf{g}. \tag{A18}$$

For, if av $(\mathbf{N})$ were not a multiple of $\mathbf{g}$, it would have different eigenvalues, the largest of which would indicate a preferred orientation. If we substitute eqn. (A18) in eqn. (A17) and use

$$\mathbf{N}_s = \mathbf{D}_s\mathbf{D}_s^{\mathrm{T}}/\det\mathbf{D}_s$$

then

$$\text{av}(\mathbf{N}_f) = J\mathbf{N}_s. \tag{A19}$$

But since $\det \mathbf{N}_s = 1$ by definition,

$$J^2 = \det(\text{av}(\mathbf{N}_f)). \tag{A20}$$

We can re-express this using eqn. (A10) as

$$\mathbf{P}_s = \frac{1}{J}\,\text{av}(\mathbf{P}_f) \tag{A21}$$

where $\mathbf{P}$ is the position vector of an ellipse on the plot. Expanding eqn. (A20) gives

$$J^2 = [\text{av}(\sqrt{1 + X_f^2 + Y_f^2})]^2 - [\text{av}\, X_f]^2 - [\text{av}\, Y_f]^2. \tag{A22}$$

J is the same for a given distribution, whatever the strain (from eqns. A18 and A20). In particular, for a random distribution,

$$\text{av}(\mathbf{P}_i) = 0 \tag{A23}$$

so

$$J = \text{av}(\sqrt{1 + X_i^2 + Y_i^2}) \tag{A24}$$

$$= \text{av}(\cosh \eta_i) = \tfrac{1}{2}\,\text{av}(R_i + 1/R_i). \tag{A25}$$

In the undeformed state, J is a measure of the spread in R values, having a minimum value of 1 when all are circles. Because of this, and its independence from strain, it is a 'distribution spread invariant'.

Finally, consider the behaviour of bedding. It might be thought that a bedding plane could be represented by an ellipse infinitely flattened in that plane, and hence by a point at radial infinity on the plot. In this case, the plane initially at $\theta_i = 45°$ would move with the asymptotes of the hyperbolae (eqn. A13). So we would have

$$\tan\alpha = \frac{1}{X_s} = \frac{1}{\sinh \eta_s} = \frac{2R_s}{R_s^2 - 1} \tag{A26}$$

which can indeed be shown to be the same as Harkers' formulae for $\theta_i = 45°$,

$$\tan\theta = 1/R_s. \tag{A27}$$

The asymptotes to the grid hyperbolae are indicated by ticks round the edge of the grid (Fig. 2).

Algol 68 procedures to draw grids, plots and manipulate ellipse data, and draw onion sets are available on request. A4 size enlargements of Fig. 2. are also available.